J|A|C|S
ARTICLES
Published on Web 11/18/2003

Cluster-to-Metal Magnetic Coupling: Synthesis and Characterization of 25-Electron $[Re_{6-n}Os_nSe_8(CN)_6]^{(5-n)-}$ ($n = 1, 2$) Clusters and $\{Re_{6-n}Os_nSe_8[CNCu(Me_6tren)]_6\}^{9+}$ ($n = 0, 1, 2$) Assemblies

Eric G. Tulsky,[†] Nathan R. M. Crawford,[†] Stéphane A. Baudron,[‡] Patrick Batail,[‡] and Jeffrey R. Long*[,†]

Contribution from the Department of Chemistry, University of California, Berkeley, California 94720-1460, and Laboratoire Chimie Inorganique, Matériaux et Interfaces, FRE 2447 CNRS, Université d'Angers, Bldg. K, 2 Boulevard Lavoisier, 49045 Angers, France

Received July 22, 2003; E-mail: jlong@cchem.berkeley.edu

Abstract: The first face-capped octahedral clusters with 25 metal-based valence electrons are shown to provide versatile building units capable of engaging in magnetic exchange coupling. Reactions of $[Re_5OsSe_8Cl_6]^{3-}$ and $[Re_4Os_2Se_8Cl_6]^{2-}$ with NaCN in a melt of $NaNO_3$ or KCF_3SO_3 afford the 24-electron clusters $[Re_5OsSe_8(CN)_6]^{3-}$ and $[Re_4Os_2Se_8(CN)_6]^{2-}$. The ^{13}C NMR spectrum of a ^{13}C-labeled version of the latter species indicates a 1:2 mixture of cis and trans isomers. Cyclic voltammograms of the clusters in acetonitrile display reversible $[Re_5OsSe_8(CN)_6]^{3-/4-}$, *cis*-$[Re_4Os_2Se_8(CN)_6]^{2-/3-}$, and *trans*-$[Re_4Os_2Se_8(CN)_6]^{2-/3-}$ couples at $E_{1/2} = -1.843$, -0.760, and -1.031 V vs $FeCp_2^{0/+}$, respectively, in addition to other redox processes. Accordingly, reduction of $[Re_5OsSe_8(CN)_6]^{3-}$ with sodium amalgam and $[Re_4Os_2Se_8(CN)_6]^{2-}$ with cobaltocene produces the 25-electron clusters $[Re_5OsSe_8(CN)_6]^{4-}$ and $[Re_4Os_2Se_8(CN)_6]^{3-}$. EPR spectra of these $S = {}^1/_2$ species in frozen DMF solutions exhibit isotropic signals with $g = 1.46$ for the monoosmium cluster and $g = 1.74$ and 1.09 for the respective cis and trans isomers of the diosmium cluster. In each case, results from DFT calculations show the unpaired spin to delocalize to some extent into the π^* orbitals of the cyanide ligands, suggesting the possibility of magnetic superexchange. Reaction of $[Re_5OsSe_8(CN)_6]^{3-}$ with $[Ni(H_2O)_6]^{2+}$ in aqueous solution generates the porous Prussian blue analogue $Ni_3[Re_5OsSe_8(CN)_6]_2 \cdot 32H_2O$; however, the tendency of the 25-electron clusters to oxidize in water prohibits their use in reactions of this type. Instead, a series of cyano-bridged assemblies, $\{Re_{6-n}Os_nSe_8[CNCu(Me_6tren)]_6\}^{9+}$ ($n = 0$, 1, 2; Me_6tren = tris(2-(dimethylamino)ethyl)amine), were synthesized to permit comparison of the exchange coupling abilities of clusters with 23−25 electrons. As expected, the results of magnetic susceptibility measurements show no evidence for exchange coupling in the assemblies containing the 23- and 24-electron clusters, but reveal the presence of weak ferromagnetic coupling in $\{Re_4Os_2Se_8[CNCu(Me_6tren)]_6\}^{9+}$. Assuming all cluster−$Cu^{II}$ exchange interactions to be equivalent, the data were fit to give an estimated coupling strength of $J = 0.4$ cm^{-1}. To our knowledge, the ability of such clusters to participate in magnetic exchange coupling has never previously been demonstrated.

Introduction

Over the past several decades, compounds containing face-capped octahedral M_6X_8 (M = second- or third-row transition metal, X = halogen or chalcogen) clusters have been investigated for a variety of potential applications.[1] The best-known such compounds are the Chevrel phases, in which $[Mo_6Q_8]^{x-}$ (Q = S, Se, Te; $x = 0-4$) cluster cores are directly interlinked to form a three-dimensional solid.[2] Soluble molecular analogues of these clusters can sometimes be isolated if an outer ligand is provided, as with the syntheses of $[Mo_6Cl_{14}]^{2-}$,[3] $[Mo_6S_8(PEt_3)_6]$,[4] $[W_6S_8(py)_6]$,[5] and $[Re_6Se_8I_6]^{4-}$.[6] In particular, cyano-ligated species of the type $[Re_6Q_8(CN)_6]^{3-/4-}$ have been of recent interest, owing to their ability to serve as bridging units in the solution-based assembly of coordination solids.[7−10] Thus, for example, the reaction between $[Ga(H_2O)_6]^{3+}$ and $[Re_6Se_8(CN)_6]^{4-}$ in aqueous solution generates a three-dimensional solid, $Ga_4[Re_6Se_8(CN)_6]_3 \cdot 38H_2O$, corresponding to an expanded analogue of Prussian blue ($Fe_4[Fe(CN)_6]_3 \cdot 14H_2O$).[9b] This compound retains its cubic framework structure upon dehydration and, by virtue of its sizable cluster components, behaves as a molecular sieve with substantial porosity.[9be] A similar approach has been used to synthesize materials exhibiting a vapochromic response[9c] or enhanced ion-exchange properties.[9d]

A further potential application for clusters of this type lies in the synthesis of a microporous magnet. Such a solid might be of utility in performing magnetic separations, since paramagnetic molecules should be preferentially absorbed over diamagnetic molecules. To date, however, only a few compounds with a truly porous framework are known to exhibit

[†] University of California at Berkeley.
[‡] Université d'Angers.

long-range magnetic order,[11] and of these just one, $Co_3[Co(CN)_5]_2$ (T_N = 38 K), has been shown to display magnetic hysteresis.[11g] The synthesis of a Prussian blue analogue incorporating paramagnetic clusters seems a fitting approach to the problem for two reasons. First, the ability to adjust the magnetic properties of Prussian blue type solids through transition metal ion substitutions is well-documented and has enabled the design of bulk magnetic materials with ordering temperatures as high as 376 K.[12] Second, cluster-expanded Prussian blue analogues form readily and are sufficiently porous to absorb sizable guest molecules.[9be] Putting this idea into practice of course requires a paramagnetic cluster unit in which the spin density is sufficiently delocalized onto the outer cyanide ligands to permit exchange coupling with neighboring metal centers.

Metal−metal bonding within face-capped octahedral clusters engenders a preference for a total of 24 metal-based valence electrons, corresponding to one bonding electron pair per edge of the M_6 octahedron.[13] Consequently, high-temperature solid-state assembly reactions generate hexarhenium clusters of this type with rhenium in exclusively the +3 oxidation state. With a sufficiently low core charge, however, the clusters can be oxidized in solution, as accomplished, for example, with the reaction between $[Re_6Se_8(CN)_6]^{4-}$ and iodine in methanol to give the paramagnetic 23-electron cluster $[Re_6Se_8(CN)_6]^{3-}$.[9e] In aqueous solution, the latter species indeed reacts with $[Ni(H_2O)_6]^{2+}$ to form a microporous Prussian blue analogue, $Ni_3[Re_6Se_8(CN)_6]_2 \cdot 33H_2O$, wherein each $S = {}^1/_2$ cluster is linked through cyanide to six $S = 1$ Ni^{II} centers.[9e] Unfortunately, the magnetic behavior of this solid reveals no signs of magnetic exchange coupling at temperatures down to 5 K. The result is consistent with the expected symmetry of the e_g HOMOs of the 24-electron cluster, as initially indicated by calculations performed on $[Mo_6S_8]^{4-}$.[13] Therein, the orbital character at each metal center exhibits δ-type symmetry with respect to the outer ligands, such that no spin density from an oxidized cluster core extends into the σ- or π-type orbitals of the cyanide ligands. Accordingly, superexchange through cyanide ligands to transition metals should be negligible for paramagnetic clusters with 21−23 metal-based valence electrons.[14] Instead, electronic structure calculations indicate that electron counts of less than 20 or greater than 24 will likely be required for achieving cluster-to-metal magnetic coupling.[13] While a few hexacyanide clusters with low electron counts have been synthesized, such as $[Mo_6Se_8(CN)_6]^{6-/7-}$ (20/21 electrons)[15] and $[W_6S_8(CN)_6]^{6-}$ (20 electrons),[16] none have yet been isolated with fewer than 20 electrons.

The particularly rigid preference of hexarhenium clusters for a precise count of 24 metal-based valence electrons makes isoelectronic core atom substitutions possible. Hence, dimensional reduction[17] of the solids $Re_6Q_8Cl_2$ (Q = S, Se) composed of interlinked $[Re_6Q_8]^{2+}$ cluster cores can be accomplished either by formal replacement of Q^{2-} with Cl^- to form $[Re_6Q_{8-n}Cl_n]^{(2+n)+}$ (n = 1, 2, 3, 4) cores[18] or by substitution of Os^{IV} for Re^{III} to form $[Re_{6-n}Os_nSe_8]^{(2+n)+}$ (n = 1, 2, 3) cores.[19] In each case, as n increases, the more positive charge on the 24-electron cluster core facilitates reduction. Accordingly, a quasireversible reduction wave appears in the cyclic voltammogram of $[Re_6S_5Cl_9]^-$,[18b] and the reversible one-electron reduction waves in the cyclic voltammograms of $[Re_{6-n}Os_nSe_8(PEt_3)_6]^{(2+n)+}$ (n = 0, 1, 2) clusters occur at potentials that become less negative with increasing n.[19] Isolation and characterization of a 25-electron cluster of this type, however, is heretofore unknown.[20]

Herein, we report the syntheses of $[Re_5OsSe_8(CN)_6]^{4-}$ and $[Re_4Os_2Se_8(CN)_6]^{3-}$, the first such 25-electron clusters, and

(1) (a) Marezio, M.; Dernier, P. D.; Remeika, J. P.; Corenzwi, E.; Matthias, B. T. *Mater. Res. Bull.* **1973**, *8*, 657. (b) Fischer, O. *Appl. Phys.* **1978**, *16*, 1. (c) Gray, H. B.; Maverick, A. W. *Science* **1981**, *214*, 1201. (d) Ekman, M. E.; Anderegg, J. W.; Schrader, G. L. *J. Catal.* **1989**, *117*, 246. (e) Pénicaud, A.; Boubekeur, K.; Batail, P.; Canadell, E.; Auban-Senzier, P.; Jérome, D. *J. Am. Chem. Soc.* **1993**, *115*, 4101. (f) Golden, J. H.; Deng, H. B.; DiSalvo, F. J.; Fréchet, J. M. J.; Thompson, P. M. *Science* **1995**, *268*, 1463. (g) Franolic, J. D.; Long, J. R.; Holm, R. H. *J. Am. Chem. Soc.* **1995**, *117*, 8139. (h) Hilsenbeck, S. J.; McCarley, R. E.; Goldman, A. I.; Schrader, G. L. *Chem. Mater.* **1998**, *10*, 125. (i) Caillat, T.; Fleurial, J. P. *J. Phys. Chem. Solids* **1998**, *59*, 1139. (j) Nunes, R. W.; Maxin, I. I.; Singh, D. J. *Phys. Rev. B* **1999**, *59*, 7969. (k) Deluzet, A.; Batail, P.; Misaki, Y.; Auban-Senzier, P.; Canadell, E. *Adv. Mater.* **2000**, *12*, 436. (l) Jin, S.; Venkataraman, D.; DiSalvo, F. J. *Inorg. Chem.* **2000**, *39*, 2747. (m) Kobayashi, N.; Ishizaka, S.; Yoshimura, T.; Kim, H.-B.; Sasaki, Y.; Kitamura, N. *Chem. Lett.* **2000**, 234. (n) Roland, B. K.; Selby, H. D.; Carducci, M. D.; Zheng, Z. *J. Am. Chem. Soc.* **2002**, *124*, 3222. (o) Gray, T. G.; Ruzinski, C. M.; Meyer, E. E.; Holm, R. H.; Nocera, D. G. *J. Am. Chem. Soc.* **2003**, *125*, 4755.

(2) (a) Chevrel, R.; Sergent, M.; Prigent, J. *J. Solid State Chem.* **1971**, *3*, 515. (b) Sergent, M.; Chevrel, R. *J. Solid State Chem.* **1973**, *3*, 433. (c) Chevrel, R.; Sergent, M.; Fischer, Ø. *Mater. Res. Bull.* **1975**, *10*, 1169. (d) Potel, M.; Gougeon, P.; Chevrel, R.; Sergent, M. *Rev. Chim. Miner.* **1984**, *21*, 509.

(3) Vaughan, P. A. *Proc. Natl. Acad. Sci. U.S.A.* **1950**, *36*, 461.

(4) Saito, T.; Yamamoto, N.; Yamagata, T.; Imoto, H. *J. Am. Chem. Soc.* **1988**, *110*, 1646.

(5) Zhang, X.; McCarley, R. E. *Inorg. Chem.* **1995**, *34*, 2678.

(6) Long, J. R.; McCarty, L. S.; Holm, R. H. *J. Am. Chem. Soc.* **1996**, *118*, 4603.

(7) Mironov, Y. V.; Cody, J. A.; Albrecht-Schmitt, T. E.; Ibers, J. A. *J. Am. Chem. Soc.* **1997**, *119*, 493.

(8) (a) Naumov, N. G.; Virovets, A. V.; Sokolov, M. N.; Artemkina, S. B.; Fedorov, V. E. *Angew. Chem., Int. Ed.* **1998**, *37*, 1943. (b) Naumov, N. G.; Artemkina, S. B.; Virovets, A. V.; Fedorov, V. E. *Solid State Sci.* **1999**, *1*, 473. (c) Naumov, N. G.; Virovets, A. V.; Fedorov, V. E. *Inorg. Chem. Commun.* **2000**, *3*, 71. (d) Artemkina, S. B.; Naumov, N. G.; Virovets, A. V.; Gromilov, S. A.; Fenske, D.; Fedorov, V. E. *Inorg. Chem. Commun.* **2001**, *4*, 423.

(9) (a) Beauvais, L. G.; Shores, M. P.; Long, J. R. *Chem. Mater.* **1998**, *10*, 3783. (b) Shores, M. P.; Beauvais, L. G.; Long, J. R. *J. Am. Chem. Soc.* **1999**, *121*, 775. (c) Beauvais, L. G.; Shores, M. P.; Long, J. R. *J. Am. Chem. Soc.* **2000**, *122*, 2763. (d) Bennett, M. V.; Shores, M. P.; Beauvais, L. G.; Long, J. R. *J. Am. Chem. Soc.* **2000**, *122*, 6664. (e) Bennett, M. V.; Beauvais, L. G.; Shores, M. P.; Long, J. R. *J. Am. Chem. Soc.* **2001**, *123*, 8022.

(10) (a) Kim, Y.; Park, S.-M.; Nam, W.; Kim, S.-J. *Chem. Commun.* **2001**, 1470. (b) Kim, Y.; Park, S.-M.; Kim, S.-J. *Inorg. Chem. Commun.* **2002**, *5*, 592. (c) Kim, Y.; Choi, S. K.; Park, S.-M.; Nam, W.; Kim, S.-J. *Inorg. Chem. Commun.* **2002**, *5*, 612.

(11) (a) Cavellec, M.; Riou, D.; Ninlaus, C.; Grenèche, J.-M.; Férey, G. *Zeolites* **1996**, *17*, 250. (b) Cavellec, M.; Riou, D.; Grenèche, J.-M.; Férey, G. *J. Magn. Magn. Mater.* **1996**, *163*, 173. (c) Zhang, X. X.; Chui, S. S.-Y.; Williams, I. D. *J. Appl. Phys.* **2000**, *87*, 6007, (d) Guillou, N.; Gao, Q.; Forster, P. M.; Chang, J.-S.; Noguès, M.; Park, S.-E.; Férey, G.; Cheetham, A. K. *Angew. Chem., Int. Ed.* **2001**, *40*, 2831. (e) Rujiwatra, A.; Kepert, C. J.; Claridge, J. B.; Rosseinsky, M. J.; Kumagai, H.; Kurmoo, M. *J. Am. Chem. Soc.* **2001**, *123*, 10584. (f) Barthelet, K.; Marrot, J.; Riou, D.; Férey, G. *Angew. Chem., Int. Ed.* **2002**, *41*, 281. (g) Beauvais, L. G.; Long, J. R. *J. Am. Chem. Soc.* **2002**, *124*, 12096. (h) Maspoch, D.; Ruiz-Molina, D.; Wurst, K.; Domingo, N.; Cavallini, M.; Biscarini, F.; Tejada, J.; Rovira, C.; Veciana, J. *Nat. Mater.* **2003**, *2*, 190.

(12) (a) Mallah, T.; Thiébaut, S.; Verdaguer, M.; Veillet, P. *Science* **1993**, *262*, 1554. (b) Entley, W. R.; Girolami, G. S. *Science* **1995**, *268*, 397. (c) Ferlay, S.; Mallah, T.; Ouahès, R.; Veillet, P.; Verdaguer, M. *Nature* **1995**, *378*, 701. (d) Dujardin, E.; Ferlay, S.; Phan, X.; Desplanches, C.; Cartier dit Moulin, C.; Sainctavit, P.; Baudelet, F.; Dartyge, E.; Veillet, P.; Verdaguer, M. *J. Am. Chem. Soc.* **1998**, *120*, 11347. (e) Holmes, S. M.; Girolami, G. S. *J. Am. Chem. Soc.* **1999**, *121*, 5593.

(13) (a) Hughbanks, T.; Hoffmann, R. *J. Am. Chem. Soc.* **1983**, *105*, 1150. (b) Hughbanks, T. *Prog. Solid State Chem.* **1989**, *19*, 329. (c) Lin, Z.; Williams, I. D. *Polyhedron* **1996**, *15*, 3277.

(14) (a) Entley, W. R.; Treadway, C. R.; Girolami, G. S. *Mol. Cryst. Liq. Cryst.* **1995**, *273*, 153. (b) Weihe, H.; Güdel, H. *Comments Inorg. Chem.* **2000**, *22*, 75.

(15) Mironov, Y. V.; Virovets, A. V.; Naumov, N. G.; Ikorskii, V. N.; Fedorov, V. E. *Chem.—Eur. J.* **2000**, *6*, 1361.

(16) Jin, S.; DiSalvo, F. J. *Chem. Commun.* **2001**, *17*, 1586.

(17) Tulsky, E. G.; Long, J. R. *Chem. Mater.* **2001**, *13*, 1149.

(18) (a) Leduc, L.; Perrin, A.; Sergent, M. *C. R. Acad. Sci., Ser. 2* **1983**, *296*, 961. (b) Gabriel, J.-C.; Boubekeur, K.; Batail, P. *Inorg. Chem.* **1993**, *32*, 2894. (c) Gabriel, J.-C. P.; Boubekeur, K.; Uriel, S.; Batail, P. *Chem. Rev.* **2001**, *101*, 2037 and references therein.

(19) Tulsky, E. G.; Long, J. R. *Inorg. Chem.* **2001**, *40*, 6990.

demonstrate that the latter species is capable of engaging in ferromagnetic exchange interactions in the hexacopper(II) assembly $\{Re_4Os_2Se_8[CNCu(Me_6tren)]_6\}^{9+}$ (Me_6tren = tris(2-(dimethylamino)ethyl)amine).

Experimental Section

Preparation of Compounds. The compounds $(Bu_4N)_3[Re_6Se_8(CN)_6]$,[9e] $Cs_3Re_5OsSe_8Cl_6$,[19] and $Cs_2Re_4Os_2Se_8Cl_6$[19] were prepared as described previously. Synthesis of $[(Me_6tren)Cu(CF_3SO_3)](CF_3SO_3)$ was carried out analogously to previous reports,[21] starting from $Cu(CF_3SO_3)_2$. Water was distilled and deionized with a Milli-Q filtering system. Pyrex ampules (with dimensions i.d. × o.d. × l = 10 × 12 × 85 mm) and $NaNO_3$ (Fisher, 99.9%) were dried for 2 days at 150 °C prior to use. Other reagents, including NaCN (Aldrich, 99.99%), and solvents were used as purchased. The loading of ampules and the preparation and handling of reduced clusters were all performed under a dinitrogen atmosphere. High-temperature reactions were carried out in tube furnaces equipped with programmable controllers; temperatures were measured near the reactants and were typically ramped up at a rate of 1 °C/min.

$(Bu_4N)_3[Re_5OsSe_8(CN)_6]$ (1). A Pyrex ampule was loaded with $Cs_3Re_5OsSe_8Cl_6$ (0.15 g, 0.063 mmol), NaCN (0.060 g, 1.2 mmol), and $NaNO_3$ (0.30 g, 3.5 mmol), evacuated, and sealed. The ampule was heated at 320 °C for 12 h, allowed to cool to ca. 200 °C, and air-quenched. The resulting orange solid was dissolved in 50 mL of water and filtered. Addition of $(Bu_4N)I$ (0.20 g, 0.54 mmol) to the filtrate caused immediate formation of an orange precipitate, which was collected by centrifugation and decantation, washed with two successive 40-mL aliquots of water, and dried in air. Recrystallization by diffusing ether vapor into an acetonitrile solution afforded red rod-shaped crystals. The supernatant solution was decanted, and the crystals were washed with 10 mL of ether and dried in air to yield 0.15 g (85%) of product. Absorption spectrum (MeCN): λ_{max} (ϵ_M) 242 (34960), 329 (4662), 452 (sh, 610), 529 (220) nm. IR (ν(CN)): 2127 (sh), 2119 cm^{-1}. ES^--MS: m/z 1076.192 ($[\mathbf{1} - 2Bu_4N]^{2-}$). Anal. Calcd for $C_{54}H_{108}N_9OsRe_5Se_8$: C, 24.60; H, 4.13; N, 4.78. Found: C, 24.57; H, 4.21; N, 4.63. Analogous reactions employing $(PPh_4)Br$ in place of $(Bu_4N)I$ resulted in crystals of $(PPh_4)_3[Re_5OsSe_8(CN)_6]$ (**1′**) suitable for X-ray analysis. Reactions employing $K^{13}CN$ (0.078 g, 1.2 mmol) in place of NaCN afforded 0.16 g (90%) of $(Bu_4N)_3[Re_5OsSe_8(^{13}CN)_6]$ (^{13}C-**1**). IR (ν(CN)): 2080 (sh), 2073 cm^{-1}. ^{13}C NMR (DMSO): 112.9 (1), 111.6 (4.00), 97.0 (0.96) ppm.

$Na_3[Re_5OsSe_8(CN)_6]$ (2). A solution of **1** (0.10 g, 0.038 mmol) in 10 mL of acetonitrile was added to a solution of NaSCN (0.030 g, 0.37 mmol) in 5 mL of acetonitrile, causing immediate formation of a yellow precipitate. The solid was collected by centrifugation and decantation, washed with successive 20-mL aliquots of acetonitrile and ether, and dried in air to yield 0.065 g (94%) of product. IR (ν(CN)): 2126 cm^{-1}. Anal. Calcd for $C_6N_6Na_3OsRe_5Se_8$: C, 3.64; H, 0.00; N, 4.25. Found: C, 3.52; H, <0.3; N, 4.21.

$(Bu_4N)_2[Re_4Os_2Se_8(CN)_6]$ (3). A Pyrex ampule was loaded with $Cs_2Re_4Os_2Se_8Cl_6$ (0.15 g, 0.067 mmol), NaCN (0.028 g, 0.57 mmol), and KCF_3SO_3 (0.30 g, 1.6 mmol), evacuated, and sealed. The ampule was heated at 330 °C for 12 h, allowed to cool to ca. 200 °C, and air-quenched. The resulting orange-brown solid was stirred in 40 mL of water for 1 h, and the orange solution was collected by centrifugation and decantation. The residual solid was stirred in an additional 40 mL of water for 1 h, and the yellow solution was again collected by centrifugation and decantation. The aqueous solutions were combined, and $(Bu_4N)I$ (0.15 g, 0.42 mmol) was added to give an immediate yellow precipitate, which was collected by centrifugation and decantation and washed with two successive 40-mL aliquots of water. The solid was extracted into 5 mL of dichloromethane; diffusion of ether vapor into this solution afforded red-brown rod-shaped crystals. The supernatant solution was decanted, and the crystals were washed with 10 mL of ether and dried in air to yield 0.14 g (89%) of product. Absorption spectrum (MeCN): λ_{max} (ϵ_M) 250 (30 800), 322 (sh, 5250), 368 (sh, 2780), 433 (sh, 982) nm. IR (ν(CN)): 2133, 2129 (sh) cm^{-1}. ES^--MS: m/z 957.54 ($[\mathbf{3} - 2Bu_4N]^{2-}$). Anal. Calcd for $C_{38}H_{72}N_8Os_2Re_4Se_8$: C, 19.03; H, 3.03; N, 4.67. Found: C, 18.95; H, 3.07; N, 4.63. Analogous reactions employing $(PPh_4)Br$ in place of $(Bu_4N)I$, followed by ether diffusion into a DMF solution, afforded crystals of $(PPh_4)_2[Re_4Os_2Se_8(CN)_6]\cdot$DMF (**3′**) suitable for X-ray analysis.

$(Bu_4N)_2[Re_4Os_2Se_8(^{13}CN)_6]$ (^{13}C-3). A Pyrex ampule was loaded with $Cs_2Re_4Os_2Se_8Cl_6$ (0.032 g, 0.013 mmol), $K^{13}CN$ (0.012 g, 0.18 mmol), and $NaNO_3$ (0.30 g, 3.5 mmol), evacuated, and sealed. The ampule was heated at 320 °C for 32 h, cooled rapidly to 200 °C, and air-quenched. The resulting yellow solid was dissolved in 30 mL of water and filtered. Addition of $(Bu_4N)I$ (0.050 g, 0.14 mmol) caused immediate formation of a yellow precipitate, which was collected by centrifugation and decantation, washed with two successive 40-mL aliquots of water, and dried briefly in air. Elution with 6:1 CH_2Cl_2−CH_3CN on a silica column (70−230 mesh silica, 5 mm diameter, 50 mm height) permitted removal of a small amount of a fast-moving yellow initial fraction; the yellow-orange second fraction was collected, and the solvent was removed on a rotary evaporator. Diffusing ether vapor into a concentrated dichloromethane solution afforded red-brown rod-shaped crystals. The supernatant solution was decanted, and the crystals were washed with 5 mL of ether and dried in air to yield 0.020 g (64%) of product. IR (ν(CN)): 2087 (sh), 2082 cm^{-1}. ^{13}C NMR (DMSO): cis, 108.7 (1), 107.8 (1.14), 92.4 (0.97); trans, 107.9 (4.12), 93.5 (2) ppm.

$Na(Bu_4N)_3[Re_5OsSe_8(CN)_6]$ (4). A solution of **1** (0.050 g, 0.019 mmol) in 5 mL of acetonitrile was added to a solution of Na (0.80 mg, 0.032 mmol) in 0.3 mL of Hg, inducing a rapid color change from orange to olive green. The solution was swirled with the sodium amalgam for 5 min and was then decanted upon allowing the amalgam to settle. Ether (ca. 10 mL) was added until an olive-green solid precipitated. The solid was collected by centrifugation and decantation, washed with ether, and dried under flowing dinitrogen to yield 0.047 g (93%) of product. Recrystallization by diffusing ether vapor into an acetonitrile solution afforded green plate-shaped crystals suitable for X-ray analysis. Absorption spectrum (MeCN): λ_{max} (ϵ_M) 283 (sh, 18 300), 363 (5370), 575 (sh, 441), 653 (sh, 348), 918 (273). IR (ν(CN)): 2094 cm^{-1}. Anal. Calcd for $C_{54}H_{108}N_9NaOsRe_5Se_8$: C, 24.4; H, 4.1; N, 4.7. Found: C, 25.0; H, 4.4; N, 4.9.

$(Bu_4N)_2(Cp_2Co)[Re_4Os_2Se_8(CN)_6]$ (5). A solution of **3** (0.075 g, 0.031 mmol) in 3 mL of dichloromethane was added to a solution of Cp_2Co (0.0068 g, 0.036 mmol) in 0.5 mL of dichloromethane and stirred for 5 min, causing precipitation of an olive-green solid. The pale green supernatant solution was decanted, and the solid was washed with successive aliquots of ether (2 × 10 mL), dried under dinitrogen, and dissolved in a minimum volume of acetonitrile. Filtration and recrystallization by ether vapor diffusion afforded olive-green rod-shaped crystals. The supernatant solution was decanted, and the crystals were washed with 10 mL of ether and dried under flowing dinitrogen to yield 0.068 g (85%) of product. Absorption spectrum (MeCN): λ_{max} (ϵ_M) 326 (sh, 22 700), 364 (sh, 10540), 500 (sh, 1040), 660 (434), 849 (461). IR (ν(CN)): 2113 cm^{-1}. Analogous reactions employing $(PPh_4)_2[Re_4Os_2Se_8(CN)_6]$ in place of $(Bu_4N)_2[Re_4Os_2Se_8(CN)_6]$, followed by ether diffusion into a DMF solution yielded dark green rod-shaped crystals of $(PPh_4)_2(CoCp_2)[Re_4Os_2Se_8(CN)_6]$ (**5′**) suitable for X-ray analysis.

$Ni_3[Re_5OsSe_8(CN)_6]_2\cdot 32H_2O$ (6). Solutions of **2** (0.041 g, 0.021

(20) Clusters with higher electron counts are readily formed with first-row transition metals, as in $[M_6Q_8(PR_3)_6]$ (M = Fe, Co; Q = S, Se); however, the diminished role of metal−metal bonding distinguishes these from the present class of compounds: (a) Cecconi, F.; Ghilardi, C. A.; Midollini, S. *Inorg. Chim. Acta Lett.* **1982**, *64*, L47. (b) Agresti, A.; Bacci, M.; Cecconi, F.; Ghilardi, C. A.; Midollini, S. *Inorg. Chem.* **1985**, *24*, 689. (c) Hong, M. C.; Huang, Z. Y.; Lei, X. J.; Wei, G. W.; Kang, B. S.; Liu, H. Q. *Polyhedron* **1991**, *10*, 927. (d) Goddard, C. A.; Long, J. R.; Holm, R. H. *Inorg. Chem.* **1996**, *35*, 4347 and references therein.

(21) Ciampolini, M.; Nardi, N. *Inorg. Chem.* **1966**, *5*, 41.

Table 1. Crystallographic Data[a] for $(PPh_4)_3[Re_5OsSe_8(CN)_6]$ (**1′**), $(PPh_4)_2[Re_4Os_2Se_8(CN)_6]\cdot$DMF (**3′**), $Na(Bu_4N)_3[Re_5OsSe_8(CN)_6]$ (**4**), and $(PPh_4)_2(CoCp_2)[Re_4Os_2Se_8(CN)_6]$ (**5′**)

	1′	3′	4	5′
formula	$C_{78}H_{60}N_6OsP_3Re_5Se_8$	$C_{57}H_{46}N_7OOs_2P_2Re_4Se_8$	$C_{54}H_{108}N_9NaOsRe_5Se_8$	$C_{64}H_{50}CoN_6Os_2P_2Re_4Se_8$
fw	2927.11	2663.83	2659.36	2780.85
T, K	159	131	150	130
space group	$P\bar{1}$	*C*2/*c*	*C*2/*m*	$P2_1/n$
Z	2	4	2	2
a, Å	13.1760(3)	12.1936(4)	15.1987(11)	11.9445(2)
b, Å	13.4661(3)	19.5516(5)	20.0425(3)	19.8950(3)
c, Å	23.1766(5)	27.7230(3)	15.5439(9)	14.012(1)
α, deg	91.591(1)			
β, deg	91.104(1)	102.688(1)	113.895(5)	95.281(1)
γ, deg	104.474(1)			
V, Å^3	3978.7(2)	6447.9(3)	4329.1(4)	3315.57(7)
d_{calc}, g/cm^3	2.443	2.744	2.040	2.785
R_1 (wR_2),[b] %	4.08 (8.78)	4.69 (9.97)	8.69 (21.63)	4.36 (10.28)

[a] Obtained with graphite-monochromated Mo Kα ($\lambda = 0.710\ 73$ Å) radiation. [b] $R_1 = \Sigma||F_o| - |F_c||/\Sigma|F_o|$, $wR_2 = \{\Sigma[w(F_o^2 - F_c^2)^2]/\Sigma[w(F_o^2)^2]\}^{1/2}$.

Table 2. Crystallographic Data[a] for $Ni_3[Re_5OsSe_8(CN)_6]_2\cdot 32H_2O$ (**6**), $\{Re_5OsSe_8[CNCu(Me_6tren)]_6\}(CF_3SO_3)_9\cdot$14MeCN (**8**·14MeCN), and $\{Re_4Os_2Se_8[CNCu(Me_6tren)]_6\}(CF_3SO_3)_9\cdot$14MeCN (**9**·14MeCN)

	6	8·14MeCN	9·14MeCN
formula	$C_{12}H_{64}N_{12}Ni_3O_{32}Os_2Re_{10}Se_{16}$	$C_{115}H_{222}Cu_6F_{27}N_{44}O_{27}OsRe_5S_9Se_8$	$C_{115}H_{222}Cu_6F_{27}N_{44}O_{27}Os_2Re_4S_9Se_8$
Formula w	4570.66	5589.03	5593.03
T, K	293	158	132
space group	$Fm\bar{3}m$	$Pa\bar{3}$	$Pa\bar{3}$
Z	1.33	4	4
a, Å	14.14495(9)	27.1909(4)	27.2115(2)
V, Å^3	2830.12(3)	20103.5(5)	20149.2(3)
d_{calc}, g/cm^3	3.560	1.843	1.844
R_1 (wR_2),[b] %	9.60 (12.33)	6.28 (16.96)	5.93 (14.42)

[a] Obtained with graphite-monochromated Mo Kα ($\lambda = 0.710\ 73$ Å) radiation. [b] $R_1 = \Sigma||F_o| - |F_c||/\Sigma|F_o|$, $wR_2 = \{\Sigma[w(F_o^2 - F_c^2)^2]/\Sigma[w(F_o^2)^2]\}^{1/2}$.

mmol) in 2 mL of water and $NiCl_2\cdot 6H_2O$ (0.25 g, 1.1 mmol) in 2 mL of water were heated to 80 °C, combined, and held at 80 °C for 14 h. The reaction mixture was then centrifuged, and the green supernatant solution was decanted from the orange precipitate. The solid was washed with two successive 10-mL aliquots of water and then dried rapidly under flowing air to yield 0.081 g (85%) of product. IR (ν(CN)): 2175 cm^{-1}. Anal. Calcd for $C_{12}H_{64}N_{12}Ni_3O_{32}Os_2Re_{10}Se_{16}$: C, 3.15; H, 1.41; N, 3.68. Found: C, 3.23; H, 1.34; N, 3.71.

$\{Re_6Se_8[CNCu(Me_6tren)]_6\}(CF_3SO_3)_9$ (7). A solution of $(Bu_4N)_3[Re_6Se_8(CN)_6]$ (0.075 g, 0.028 mmol) in 5 mL of acetonitrile was added dropwise to a solution of $[(Me_6tren)Cu(CF_3SO_3)](CF_3SO_3)$ (0.11 g, 0.18 mmol) in 2 mL of acetonitrile. After the mixture was stirred for 5 min, 15 mL of ether was added to precipitate a dark green solid, which was collected by centrifugation and decantation, washed with 10 mL of ether, and dried in air. Diffusing ether vapor into a concentrated acetonitrile solution of the solid afforded dark green rod-shaped crystals. The supernatant solution was decanted, and the crystals were washed with ether (2 × 15 mL) and dried in vacuo to yield 0.13 g (88%) of product. Absorption spectrum (MeCN): λ_{max} (ϵ_M) 226 (64 190), 293 (51 820), 455 (sh, 1221), 643 (sh, 797), 829 (2996) nm. IR (ν(CN)): 2152 cm^{-1}. μ_{eff} (298 K): 4.34 μ_B. Anal. Calcd for $C_{87}H_{180}Cu_6F_{27}N_{30}O_{27}Re_6S_9Se_8$: C, 20.86; H, 3.62; N, 8.38. Found: C, 21.21; H, 3.91; N, 8.60.

$\{Re_5OsSe_8[CNCu(Me_6tren)]_6\}(CF_3SO_3)_9$ (8). A solution of **1** (0.075 g, 0.028 mmol) in 5 mL of acetonitrile was added dropwise to a solution of $[(Me_6tren)Cu(CF_3SO_3)](CF_3SO_3)$ (0.10 g, 0.18 mmol) in 2 mL of acetonitrile. After the mixture was stirred for 5 min, 15 mL of ether was added to precipitate a green solid, which was collected by centrifugation and decantation, washed with 10 mL of ether, and dried in air. Diffusing ether vapor into a concentrated acetonitrile solution of the solid afforded dark green cube-shaped crystals of **8**·14MeCN. The supernatant solution was decanted, and the crystals were washed with 10 mL of ether and dried in vacuo to yield 0.13 g (91%) of product. Absorption spectrum (MeCN): λ_{max} (ϵ_M) 243 (39 700), 295 (44 600), 449 (822), 539 (302), 636 (sh, 652), 835 (3050) nm. IR (ν(CN)): 2168 cm^{-1}. μ_{eff} (298 K): 4.26 μ_B. Anal. Calcd for $C_{87}H_{180}Cu_6F_{27}N_{30}O_{27}OsRe_5S_9Se_8$: C, 20.84; H, 3.62; N, 8.38. Found: C, 20.46; H, 3.73; N, 8.18.

$\{Re_4Os_2Se_8[CNCu(Me_6tren)]_6\}(CF_3SO_3)_9$ (9). A slurry of **5** (0.075 g, 0.029 mmol) in 5 mL of acetonitrile was added dropwise to a solution of $[(Me_6tren)Cu(CF_3SO_3)](CF_3SO_3)$ (0.11 g, 0.18 mmol) in 2 mL of acetonitrile. After the mixture was stirred for 5 min, 15 mL of ether was added to precipitate a dark green solid, which was collected by centrifugation and decantation, washed with 10 mL of ether, and dried under flowing dinitrogen. Diffusing ether vapor into a concentrated acetonitrile solution of the solid afforded dark-green cube-shaped crystals of **9**·14MeCN. The supernatant solution was decanted, and the crystals were washed with 10 mL of ether and dried in vacuo to yield 0.13 g (93%) of product. Absorption spectrum (MeCN): λ_{max} (ϵ_M) 250 (34 180), 294 (39 100), 641 (sh, 1115), 834 (3043) nm. IR (ν(CN)): 2166 cm^{-1}. μ_{eff} (298 K): 4.74 μ_B. Anal. Calcd for $C_{87}H_{180}Cu_6F_{27}N_{30}O_{27}Os_2Re_4S_9Se_8$: C, 20.82; H, 3.62; N, 8.37. Found: C, 21.03; H, 3.58; N, 8.30.

X-ray Structure Determinations. Single crystals of the compounds listed in Tables 1 and 2 (except for **6**) were coated with Paratone-N oil, attached to glass fibers, transferred to a Siemens SMART diffractometer, and cooled in a dinitrogen stream. Initial lattice parameters were obtained from a least-squares analysis of more than 30 centered reflections; these parameters were later refined against all data. A full hemisphere of data was collected for all compounds except **9**, for which a quadrant of data was collected. None of the crystals showed significant decay during data collection. Data were integrated and corrected for Lorentz and polarization effects using SAINT and were corrected for absorption effects using SADABS 2.3.

Space group assignments were based upon systematic absences, *E* statistics, and successful refinement of the structures. Structures were solved by direct methods with the aid of successive difference Fourier maps and were refined against all data using the SHELXTL 5.0 software package. Thermal parameters for all non-hydrogen atoms were refined anisotropically, except for the partially occupied sites associated with

disordered C and N atoms in the structures of **1′** and **3′**, which were refined isotropically. Hydrogen atoms associated with disordered carbon atoms were not included in the structural refinements. All other hydrogen atoms were assigned to ideal positions and refined using a riding model with an isotropic thermal parameter 1.2 times that of the attached carbon atom (1.5 times for methyl hydrogens). The metal sites in each cluster were assigned a mixed occupancy of 5/6 Re + 1/6 Os or 2/3 Re + 1/3 Os for the structures containing Re_5OsSe_8 or $Re_4Os_2Se_8$ clusters, respectively; in these cases, efforts to localize the metals on specific sites showed no consistent improvement in the structural refinement. Crystals of **4** are extremely air-sensitive, and the poor quality of this structure refinement is attributed to a decline in crystal quality incurred while transferring it into the dinitrogen stream. The high residual factors obtained in refining the structure of **8**·14MeCN are a consequence of poor crystal quality stemming from a partial loss of lattice solvent. The standard deviations associated with mean bond distances and angles reported herein reflect the range of these values and were calculated without incorporating the esds from the structure determinations.

High-resolution X-ray powder diffraction data were collected for compound **6** at beamline 2-1 at the Stanford Synchrotron Radiation Laboratory. A finely ground powder was loaded into a 0.5 mm glass capillary under aerobic conditions. X-rays of wavelength 1.278 04 Å were selected using a Si(111) monochromator. Data were collected in Q-space ($Q = 2\pi/d$) over the range 0.700−7.000 $Å^{-1}$ ($2\theta = 8-90°$) with 0.001 $Å^{-1}$ steps. The wavelength, zero point, and profile parameters were refined using a Si standard (NIST 640b). The crystal structure of $Ni_3[Re_6Se_8(CN)_6]_2 \cdot 33H_2O$[9e] was adopted as a starting model for Rietveld refinements against the diffraction data using the program GSAS. A cosine Fourier series background, diffuse scattering parameters, and a Lorentzian peak shape were all also refined. Locations of the oxygen atoms in solvate water molecules were determined using difference Fourier maps. Anisotropic thermal parameters were refined for the Re/Os and Se atoms, and isotropic thermal parameters were refined for the Ni atoms. The thermal parameters for C, N, and metal-bound O atoms were fixed at an isotropic value of 0.025 $Å^2$; thermal parameters for O atoms in solvate water molecules were fixed at 0.06 $Å^2$.

Other Physical Measurements. Infrared spectra were recorded on a Nicolet Avatar 360 FTIR spectrometer equipped with a horizontal attenuated total reflectance accessory, except for the reduced clusters, for which transmission mode measurements were performed on Nujol mulls. Cyclic voltammetry was performed in a 0.1 M solution of $(Bu_4N)BF_4$ in acetonitrile using a Bioanalytical systems CV-50W voltammagraph, a platinum disk working electrode, a platinum wire supporting electrode, and a silver wire reference electrode. Reported potentials are all referenced to the $[FeCp_2]^{0/+}$ couple and were determined using ferrocene as an internal standard. Magnetic susceptibility data were measured on a Quantum Design MPMS2 SQUID magnetometer. Mass spectrometric measurements were performed on a Bruker Apex II 7 T actively shielded Fourier transform ion cyclotron resonance mass spectrometer equipped with an analytical electrospray ion source instrument. NMR spectra were measured with a Bruker DRX 500 MHz instrument. EPR spectra were measured with a Bruker EMX-300 MHz instrument.

Electronic Structure Calculations. Density functional theory (DFT) calculations were performed using the NWChem 4.5 quantum chemistry software package.[22] Starting geometries were taken from crystal structures and idealized to the maximal point group symmetry of the cluster ion. Geometries for all clusters were then optimized using the HCTH/407 functional.[23] Effective core potentials including relativistic effects were employed for Re and Os (LANL2DZ) and Se (LANL2-DZdp), together with the corresponding Gaussian basis sets;[24] the 6-31+G* basis was employed for C and N. To address the negative charge of the clusters, basis sets were chosen that added diffuse and polarization functions to all non-hydrogen atoms except Re and Os. The basis sets for Re and Os were manually augmented with diffuse orbitals derived from the highest occupied angular momentum orbitals used for each atom by multiplying the lowest exponent by 0.4, and a set of f polarization functions that were taken from a previous report.[25] The Ahlrichs auxiliary basis sets were used for fitting the Coulomb potential.[26] For clusters with low-lying unoccupied orbitals or a degenerate HOMO where a Jahn−Teller distortion would be expected, the geometry was optimized with alternate orbital occupation and/or lowered symmetry to break the degeneracy.

Results and Discussion

24-Electron Hexacyanide Clusters. Although cyanide tends to form strong terminal bonds to face-capped octahedral M_6Q_8 (M = second- or third-row transition metal, Q = chalcogen) clusters, the activation energy for removing the chloride ligands from $[Re_5OsSe_8Cl_6]^{3-}$ or $[Re_4Os_2Se_8Cl_6]^{2-}$ is apparently quite high. For example, heating a DMF solution of $(Bu_4N)_3[Re_5OsSe_8Cl_6]$ and 100 equiv of NaCN at reflux for 7 days results in only partial exchange of chloride for cyanide, as probed via mass spectrometry. Higher temperatures are required for the reaction to proceed efficiently, and indeed, such substitutions have typically been accomplished using an alkali metal cyanide melt at temperatures of at least 600 °C.[7,9a,b,15,27] In the present cases, however, it was found that such treatment decomposes the rhenium−osmium clusters, affording $NaCs_3Re_6Se_8(CN)_6$[9a] as the only soluble cluster-containing product. An inert, lower melting salt was therefore sought as a reaction medium that would permit access to intermediate temperatures. At 320 °C, a sodium nitrate melt proved suitably unreactive toward the $[Re_5OsSe_8]^{3+}$ cluster core, enabling facile ligand exchange to form $[Re_5OsSe_8(CN)_6]^{3-}$ with an optimal NaCN:$NaNO_3$ ratio of 2:5 (w:w). In contrast, the $[Re_4Os_2Se_8]^{4+}$ cluster core is considerably more reactive in the melt and was only reliably maintained in reactions with NaCN:$NaNO_3$ ratios of less than 1:30. Separation of $[Re_4Os_2Se_8(CN)_6]^{2-}$ then required use of column chromatography, as described in the preparation of compound ^{13}C-**3**. Interestingly, one of the side products isolated during this procedure was an oxo-bridged dicluster, $\{[Re_4Os_2Se_8(CN)_5]_2O\}^{4-}$,[28] with a structure analogous to that previously

(22) Apra, E.; Bylaska, E. J.; de Jong, W.; Hackler, M. T.; Hirata, S.; Pollack, L.; Smith, D.; Straatsma, T. P.; Windus, T. L.; Harrison, R. J.; Nieplocha, J.; Tipparaju, V.; Kumar, M.; Brown, E.; Cisneros, G.; Dupuis, M.; Fann, G. I.; Fruchtl, H.; Garza, J.; Hirao, K.; Kendall, R.; Nichols, J. A.; Tsemekhman, K.; Valiev, M.; Wolinski, K.; Anchell, J.; Bernholdt, D.; Borowski, P.; Clark, T.; Clerc, D.; Dachsel, H.; Deegan, M.; Dyall, K.; Elwood, D.; Glendening, E.; Gutowski, M.; Hess, A.; Jaffe, J.; Johnson, B.; Ju, J.; Kobayashi, R.; Kutteh, R.; Lin, Z.; Littlefield, R.; Long, X.; Meng, B.; Nakajima, T.; Niu, S.; Rosing, M.; Sandrone, G.; Stave, M.; Taylor, H.; Thomas, G.; van Lenthe, J.; Wong, A.; Zhang, Z. *NWChem, A Computational Chemistry Package for Parallel Computers*, version 4.5; Pacific Northwest National Laboratory: Richland, WA 99352-0999, 2003.
(23) Boese, A. D.; Handy, N. C. *J. Chem. Phys.* **2001**, *114*, 5497.
(24) (a) Hay, P. J.; Wadt, W. R. *J. Chem. Phys.* **1985**, *82*, 270. (b) Wadt, W. R.; Hay, P. J. *J. Chem. Phys.* **1985**, *82*, 284. (c) Hay, P. J.; Wadt, W. R. *J. Chem. Phys.* **1985**, *82*, 299. (d) Dunning, T. H., Jr.; Hay, P. J. In *Modern Theoretical Chemistry*; Schaefer, H. F., Ed.; Plenum: New York, 1976; Vol. 3, p 1. (e) Check, C. E.; Faust, T. O.; Bailey, J. M.; Wright, B. J.; Gilbert, T. M.; Sunderlin, L. S. *J. Phys. Chem. A* **2001**, *105*, 8111.
(25) Ehlers, A. W.; Bohme, M.; Dapprich, S.; Gobbi, A.; Hollwarth, A.; Jonas, V.; Kohler, K. F.; Stegmann, R.; Veldkamp, A.; Frenking, G. *Chem. Phys. Lett.* **1993**, *208*, 111.
(26) (a) Eichkorn, K.; Treutler, O.; Ohm, H.; Haser, M.; Ahlrichs, R. *Chem. Phys. Lett.* **1995**, *240*, 283. (b) Eichkorn, K.; Weigend, F.; Treutler, O.; Ahlrichs, R. *Theor. Chim. Acc.* **1997**, *97*, 119.
(27) (a) Mironov, Y. V.; Virovets, A. V.; Fedorov, V. E.; Podberezskaya, N. V.; Shishkin, O. V.; Struchkov, Y. T. *Polyhedron* **1995**, *14*, 3171. (b) Slougui, A.; Mironov, Y. V.; Perrin, A.; Fedorov, V. E. *Croat. Chem. Acta* **1995**, *68*, 885.
(28) Tulsky, E. G.; Long, J. R. Work in progress.

Table 3. Selected Mean Interatomic Distances (Å) and Angles (deg) for the Clusters in $(Bu_4N)_3[Re_6Se_8(CN)_6]\cdot 3H_2O$,[9e] $NaCs_3[Re_6Se_8(CN)_6]$,[9a] $(PPh_4)_3[Re_5OsSe_8(CN)_6]$ (**1′**), $Na(Bu_4N)_3[Re_5OsSe_8(CN)_6]$ (**4**), $(PPh_4)_2[Re_4Os_2Se_8(CN)_6]\cdot$DMF (**3′**), and $(PPh_4)_2(CoCp_2)[Re_4Os_2Se_8(CN)_6]$ (**5′**)

	$[Re_6Se_8(CN)_6]^{3-}$	$[Re_6Se_8(CN)_6]^{4-}$	$[Re_5OsSe_8(CN)_6]^{3-}$	$[Re_5OsSe_8(CN)_6]^{4-}$	$[Re_4Os_2Se_8(CN)_6]^{2-}$	$[Re_4Os_2Se_8(CN)_6]^{3-}$
electron count	23	24	24	25	24	25
M−M	2.632(5)	2.634(4)	2.626(4)	2.648(3)	2.628(3)	2.663(7)
trans-M···M	3.72(1)	3.725(6)	3.714(6)	3.744(1)	3.716(4)	3.767(2)
M−Se	2.519(8)	2.52(1)	2.512(7)	2.517(2)	2.507(4)	2.515(8)
M−C	2.06(1)	2.10(2)	2.09(2)	2.15(3)	2.08(4)	2.10(2)
C−N	1.12(1)	1.17(1)	1.15(6)	1.12(1)	1.14(3)	1.15(2)
M−Se−M	63.0(3)	62.9(3)	63.0(1)	63.4(4)	63.2(2)	63.9(3)
Se−M−Se	89.9(4)	89.9(3)	90.0(3)	89.9(5)	89.9(3)	89.9(5)
	176.3(2)	176.3(1)	176.3(1)	175.7(3)	176.0(1)	175.1(3)
Se−M−C	92(2)	92(3)	92(2)	92.1(8)	92.0(8)	92(2)
M−C−N	178	175(2)	176.6(2)	171(3)	177(2)	179.2(2)

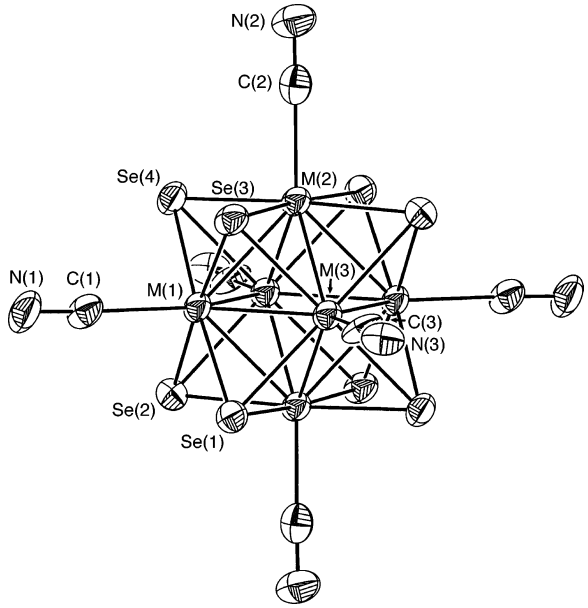

Figure 1. Structure of the 24-electron cluster $[Re_5OsSe_8(CN)_6]^{3-}$, as observed in **1′**. Ellipsoids are drawn at the 50% probability level. Atoms labeled M were modeled as 5/6 Re and 1/6 Os. The molecule resides on a crystallographic inversion center.

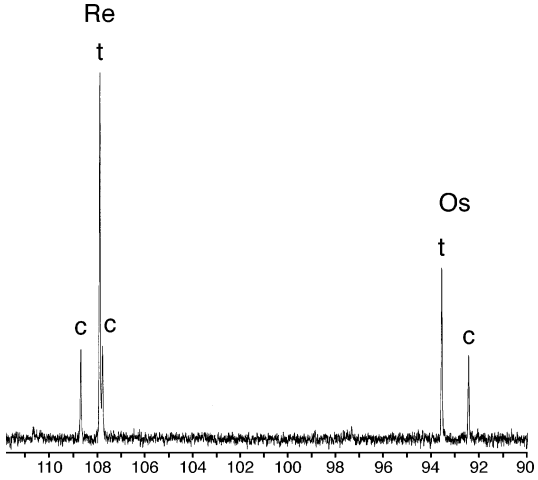

Figure 2. ^{13}C NMR spectrum of $[Re_4Os_2Se_8(CN)_6]^{2-}$, obtained for a solution of ^{13}C-**3** in DMSO. The areas under the peaks labeled "c" are in roughly a 1:1:1 ratio, consistent with the C_{2v}-symmetric cis isomer, while the peaks labeled "t" are in a 2:1 ratio, consistent with the D_{4h}-symmetric trans isomer.

encountered in $(Bu_4N)_4\{[Re_6S_5OCl_7]_2O\}$.[29] Ultimately, KCF_3SO_3 was determined to provide a more suitable medium for synthesizing $[Re_4Os_2Se_8(CN)_6]^{2-}$.

The face-capped octahedral structure of the $[Re_5OsSe_8(CN)_6]^{3-}$ cluster, as crystallized in $(PPh_4)_3[Re_5OsSe_8(CN)_6]$ (**1′**), is depicted in Figure 1. The molecule has crystallographically imposed inversion symmetry and, treating all metals as equivalent, closely approximates O_h symmetry. None of the metals feature anomalous bond lengths or angles that might indicate a preference of osmium for occupying a particular site; hence, the osmium atom is most likely disordered over all metal positions in the crystal structure. Similarly, the crystal structure of $(PPh_4)_2[Re_4Os_2Se_8(CN)_6]\cdot$DMF (**3′**) revealed no site preference for the osmium atoms. As previously observed for $[Re_{6-n}Os_nSe_8Cl_6]^{(4-n)-}$,[19] the variations in bond lengths of the 24-electron $[Re_{6-n}Os_nSe_8(CN)_6]^{(4-n)-}$ clusters (see Table 3) are consistent with predictions based on simple electrostatic arguments. Thus, with increasing positive charge on the $[Re_{6-n}Os_nSe_8]^{(2+n)+}$ cluster core, the anionic cyanide ligands are pulled in slightly, resulting in a decrease in the mean M−C distance from 2.10(2) to 2.09(2) to 2.08(4) Å for $n = 0$, 1, and 2, respectively.

Two distinct isomers are possible for the $[Re_4Os_2Se_8(CN)_6]^{2-}$ cluster: one with the osmium atoms situated at trans vertexes of the M_6 octahedron and one with them at cis vertexes. With D_{4h} symmetry, the former should give rise to a 2:1 ratio of peaks in the ^{13}C NMR spectrum, while the latter, with C_{2v} symmetry, should display a 1:1:1 ratio of peaks. The ^{13}C NMR spectrum for a concentrated DMSO solution of $(Bu_4N)_2[Re_4Os_2Se_8(^{13}CN)_6]$ is shown in Figure 2 and indeed displays precisely this 2:1 + 1:1:1 pattern. Thus, the peaks occurring at 107.9 and 93.5 ppm are assigned to the osmium- and rhenium-bound cyanide ligands in the trans cluster, respectively, and the cis:trans ratio of clusters is 1:2.0. Furthermore, in view of the comparable 15 ppm gap in the ^{13}C NMR spectrum of a DMSO solution containing $[Re_5OsSe_8(^{13}CN)_6]^{3-}$, it appears that the downfield peaks all arise from cyanide ligands bound to rhenium, while the upfield peaks correspond to those bound to osmium. Previous ^{31}P NMR experiments on solutions of $[Re_4Os_2Se_8(PEt_3)_6]^{4+}$ indicated that the trans isomer constituted approximately 55% of the mixture[19] rather than 67%. The variation between the two results could arise from a number of factors; however, since not all of the $Cs_2Re_4Os_2Se_8Cl_6$ precursor is converted into $(Bu_4N)_2[Re_4Os_2Se_8(CN)_6]$, a likely explanation is that the cis isomer is more susceptible to decomposition or

(29) Simon, F.; Boubekeur, K.; Gabriel, J.-C. P.; Batail, P. *Chem. Commun.* **1998**, 845.

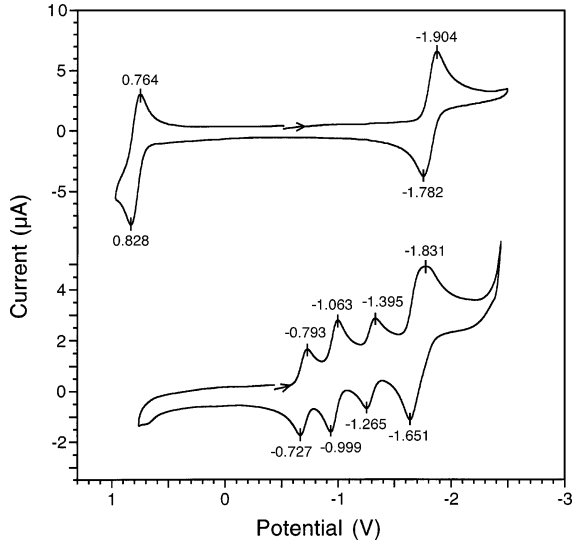

Figure 3. Cyclic voltammograms for acetonitrile solutions containing $(Bu_4N)_3[Re_5OsSe_8(CN)_6]$ (top) and $(Bu_4N)_2[Re_4Os_2Se_8(CN)_6]$ (bottom), with potentials reported versus $Cp_2Fe^{0/+}$. For the diosmium cluster, the presence of two distinct isomers leads to two sets of peaks. The smaller pair is assigned to first and second reductions of the cis isomer, while the larger pair is assigned to reduction of the trans isomer.

formation of products other than $[Re_4Os_2Se_8(CN)_6]^{2-}$ than is the trans isomer.

Figure 3 shows the cyclic voltammograms obtained for acetonitrile solutions containing $[Re_5OsSe_8(CN)_6]^{3-}$ (top) and $[Re_4Os_2Se_8(CN)_6]^{2-}$ (bottom). The former exhibits a reversible oxidation, with the $[Re_5OsSe_8(CN)_6]^{3-/2-}$ couple centered at $E_{1/2} = 0.796$ V ($\Delta E_p = 64$ mV) vs $FeCp_2^{0/+}$, as well as a reduction, with the $[Re_5OsSe_8(CN)_6]^{3-/4-}$ couple centered at $E_{1/2} = -1.843$ V ($\Delta E_p = 122$ mV). For $[Re_4Os_2Se_8(CN)_6]^{2-}$, two sets of reduction events are apparent, consistent with the presence of two distinct isomers. The two couples with lower amplitude waves are assigned to reduction of the cis isomer on the basis of its lower concentration in the ^{13}C NMR spectrum (Figure 2). These correspond to a *cis*-$[Re_4Os_2Se_8(CN)_6]^{2-/3-}$ couple centered at $E_{1/2} = -0.760$ V ($\Delta E_p = 63$ mV) and a *cis*-$[Re_4Os_2Se_8(CN)_6]^{3-/4-}$ couple centered at $E_{1/2} = -1.330$ V ($\Delta E_p = 130$ mV). The larger amplitude waves can then be attributed to a *trans*-$[Re_4Os_2Se_8(CN)_6]^{2-/3-}$ couple at $E_{1/2} = -1.031$ V ($\Delta E_p = 64$ mV) and a *trans*-$[Re_4Os_2Se_8(CN)_6]^{3-/4-}$ couple at $E_{1/2} = -1.741$ V ($\Delta E_p = 180$ mV). The appearance of the waves for this last couple suggests that they may actually incorporate an additional redox process. Note that these cyanide-terminated clusters are slightly more difficult to reduce than their triethylphosphine-ligated analogues,[19] as might be expected from the significantly more negative overall charges. In contrast to the situation here, however, the trans isomer of $[Re_4Os_2Se_8(PEt_3)_6]^{4+}$ is more easily reduced than the cis isomer.[19] It is not immediately apparent why replacing PEt_3 ligands with cyanide ligands should invert the relative ease of reduction, although it is consistent with the electronic structure calculations discussed below.

25-Electron Hexacyanide Clusters. With utilization of the cyclic voltammograms, chemical reductants were selected for producing the one-electron-reduced hexacyanide clusters. Reaction of $[Re_5OsSe_8(CN)_6]^{3-}$ with sodium amalgam was found to afford $[Re_5OsSe_8(CN)_6]^{4-}$ readily, while cobaltocene was employed in generating $[Re_4Os_2Se_8(CN)_6]^{3-}$. Both reactions

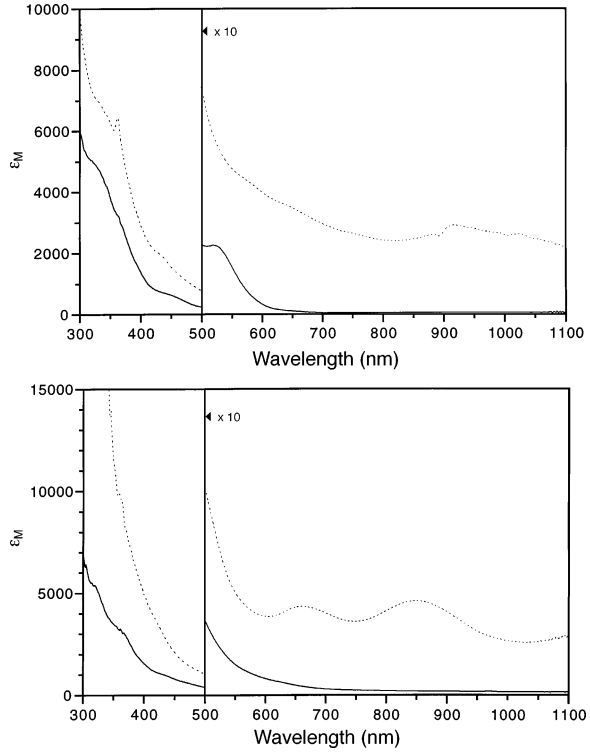

Figure 4. Top: Absorption spectra for acetonitrile solutions containing $[Re_5OsSe_8(CN)_6]^{3-}$ (solid line) and $[Re_5OsSe_8(CN)_6]^{4-}$ (dotted line). Bottom: Absorption spectra for acetonitrile solutions containing $[Re_4Os_2Se_8(CN)_6]^{2-}$ (solid line) and $[Re_4Os_2Se_8(CN)_6]^{3-}$ (dotted line).

proceed rapidly and in high yield. In each case, reduction of the cluster shifts the cyanide stretch to lower frequency in the infrared spectrum and prompts a color change from orange to olive green. The corresponding electronic absorption spectra are shown in Figure 4 and reveal several new bands arising at low energy for the 25-electron clusters. The reduced clusters decompose rapidly in air, giving orange products that presumably contain the respective 24-electron clusters. It should also be feasible to isolate the 26-electron species $[Re_4Os_2Se_8(CN)_6]^{4-}$, but like $[Re_5OsSe_8(CN)_6]^{3-}$, both of its isomers will be highly reducing and perhaps of limited utility as building units.

The structures of $Na(Bu_4N)_3[Re_5OsSe_8(CN)_6]$ (**4**) and $(PPh_4)_2(CoCp_2)[Re_4Os_2Se(CN)_6]$ (**5′**) indicate that the clusters expand somewhat upon reduction. As compared in Table 3, the 25-electron clusters exhibit slightly lengthened metal−metal bonds and metal−anion bonds relative to the 24-electron parent species. The largest differences are associated with the increased M−C separations upon reduction, which again are consistent with the change in the formal charge of the cluster cores. Previous reports on 21-electron Mo_6 and 23-electron Re_6 clusters of this type have shown that, particularly at low temperatures, significant variation in the trans metal−metal distances can arise from a Jahn−Teller distortion.[30] No such variations are observed, however, in the structures of **4** and **5′**, where the trans metal−metal distances are all identical for $[Re_5OsSe_8(CN)_6]^{4-}$ and vary only by thousandths of an Ångstrom for $[Re_4Os_2Se_8(CN)_6]^{3-}$. This could be because the osmium atoms break any degeneracy in the orbitals receiving the added electron or

(30) (a) Saito, T.; Yamamoto, N.; Nagase, T.; Tsuboi, T.; Kobayashi, K.; Yamagata, T.; Imoto, H.; Unoura, K. *Inorg. Chem.* **1990**, *29*, 764. (b) Baudron, S. A.; Deluzet, A.; Boubekeur, K.; Batail, P. *Chem. Commun.* **2002**, 2124.

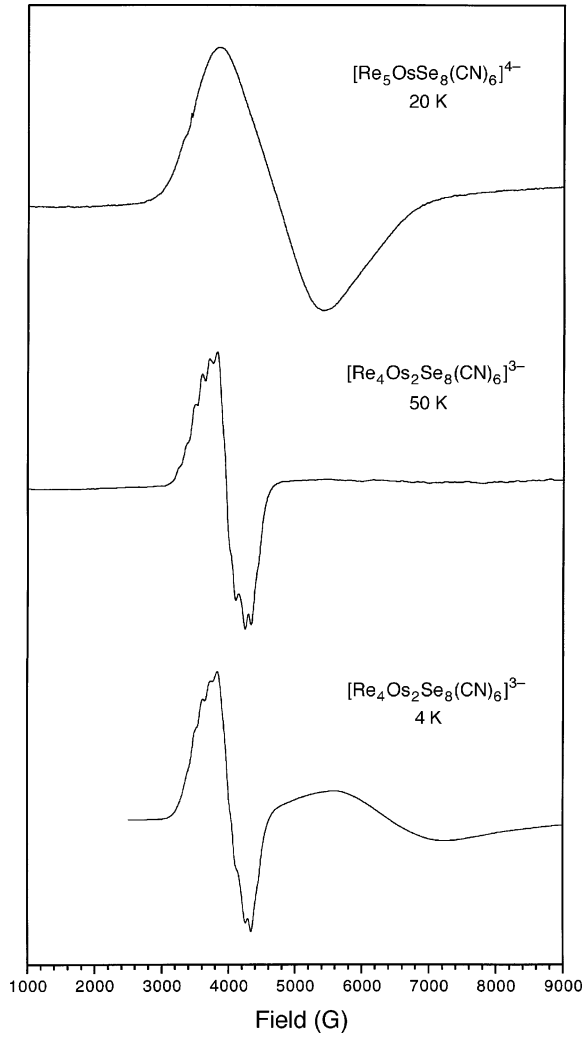

Figure 5. EPR spectra of frozen DMF solutions containing the 25-electron clusters. For $[Re_4Os_2Se_8(CN)_6]^{3-}$, two signals are observed at low temperatures; the one at lower field is attributed to the cis isomer, and the other, to the trans isomer.

because the osmium atoms enforce a preferred distortion axis in the cluster but are disordered in the crystal structure. Comparison of three clusters with identical charge but varying electron counts—23-electron $[Re_6Se_8(CN)_6]^{3-}$, 24-electron $[Re_5OsSe_8(CN)_6]^{3-}$, and 25-electron $[Re_4Os_2Se_8(CN)_6]^{3-}$—allows the effect of the electron count on the geometry to be deconvoluted from the effect of the alteration of the charge. As evident from inspection of Table 3, the metal−metal bonds are shortest in the 24-electron cluster, but the metal−carbon bonds are shortest in the 23-electron cluster.

Frozen-solution EPR spectra were measured to probe the nature of the unpaired spin in the reduced clusters (see Figure 5). A broad, featureless signal with $g = 1.46$ is observed for $[Re_5OsSe_8(CN)_6]^{4-}$, whereas $[Re_4Os_2Se_8(CN)_6]^{3-}$ gives rise to two distinct signals, consistent with the presence of cis and trans isomers. These two signals are markedly different: one, at $g = 1.74$, is sharp and shows hyperfine coupling, while the other, at $g = 1.09$, is broad, featureless, and appears only at low temperature. Thus, the values of g for the 25-electron clusters are much lower than the value of $g = 2.51$ observed for the 23-electron cluster $[Re_6Se_8I_6]^{3-}$,[31] presumably because of the spin−orbit coupling arising from the plethora of low-lying unoccupied orbitals. In the spectra of $[Re_4Os_2Se_8(CN)_6]^{3-}$, the hyperfine coupling for the signal at $g = 1.74$ results in 11 lines with a spacing of 121 G. Given the limited isotopic abundance and low magnetic moments of ^{187}Os, ^{189}Os, ^{77}Se, and ^{13}C, the most probable cause for the coupling is the interaction of the unpaired electron with two equivalent $I = 5/2$ rhenium nuclei.[32] Since all four rhenium atoms are equivalent in *trans*-$[Re_4Os_2Se_8(CN)_6]^{3-}$, this signal must be due to the C_{2v}-symmetric cis isomer. The featureless signal at $g = 1.09$ must then arise from the trans isomer.

Electronic Structure Calculations. To assess the suitability of the 25-electron clusters for engaging in magnetic exchange interactions, electronic structure calculations were performed on $[Re_5OsSe_8(CN)_6]^{4-}$ and $[Re_4Os_2Se_8(CN)_6]^{3-}$ using DFT.[33] Cluster geometries were taken from the crystal structures of **4** and **5′** and then optimized. For practical reasons, we will focus our attention on the results for the diosmium species; an energy level diagram and frontier orbital depictions for the more reactive $[Re_5OsSe_8(CN)_6]^{4-}$ cluster can be found in Figure S1 of the Supporting Information. As shown in Figure 6, the two isomers of $[Re_4Os_2Se_8(CN)_6]^{3-}$ exhibit significantly different electronic structures, with the cis isomer being 4.4 kcal/mol more stable than the trans isomer. The difference in the gas-phase reduction potentials for their 24-electron parents—calculated by subtracting the total energy of the 25-electron cluster from the total energy of the corresponding 24-electron cluster—is 0.52 eV, only slightly greater than the 0.27 V separation between isomers observed in acetonitrile solution by cyclic voltammetry (see Figure 3).

For *cis*-$[Re_4Os_2Se_8(CN)_6]^{3-}$, the unpaired electron resides in a relatively isolated b_1 orbital (here referred to as the SOMO), lying 1.7 eV above a fully occupied a_1 orbital and 0.6 eV below the b_1 LUMO. Although primarily associated with the cluster core, the SOMO places some amount of electron density in the π^* orbitals of four of the cyanide ligands. The majority of this occurs on the cyanide ligands bound to the two osmium atoms, while a much smaller amount occurs on the cyanide ligands of the two rhenium atoms that are trans to an osmium atom. Thus, one would indeed expect magnetic exchange coupling to arise if *cis*-$[Re_4Os_2Se_8(CN)_6]^{3-}$ were surrounded by six paramagnetic transition metal ions, albeit almost exclusively with the two metals coordinated by the osmium bound cyanide ligands. Assuming an octahedral coordination geometry for these metal centers, the Heisenberg exchange would be antiferromagnetic with unpaired t_{2g} electrons and ferromagnetic with unpaired e_g electrons.[14]

In the case of the *trans*-$[Re_4Os_2Se_8(CN)_6]^{3-}$ cluster, the unpaired electron resides in an orbital that is more than 2 eV above the highest fully occupied orbital but is not well-separated from the LUMO. The 24-electron parent species, *trans*-[Re_4-

(31) Zheng, Z. P.; Gray, T. G.; Holm, R. H. *Inorg. Chem.* **1999**, *38*, 4888.

(32) Coupling with rhenium nuclei can lead to splitting of this magnitude, with differences between ^{185}Re and ^{187}Re typically not resolved as a result of their very similar magnetic moments. See: (a) Dorain, P. B.; Rahn, R. *J. Chem. Phys.* **1962**, *36*, 561. (b) Rahn, R.; Dorain, P. B. *J. Chem. Phys.* **1964**, *42*, 3249.

(33) For the results of recent calculations performed on related 23- and 24-electron clusters, see:[1o,19] (a) Robinson, L. M.; Bain, R. L.; Shriver, D. F.; Ellis, D. E. *Inorg. Chem.* **1995**, *34*, 5588. (b) Arratia-Perez, R.; Hernandez-Acevedo, L. *J. Chem. Phys.* **1999**, *110*, 2529. (c) Arratia-Perez, R.; Hernandez-Acevedo, L. *J. Chem. Phys.* **1999**, *111*, 168. (d) Deluzet, A.; Duclusaud, H.; Sautet, P.; Borshch, S. A. *Inorg. Chem.* **2002**, *41*, 2537. (e) Arratia-Perez, R.; Hernandez-Acevedo, L. *J. Chem. Phys.* **2003**, *118*, 7425.

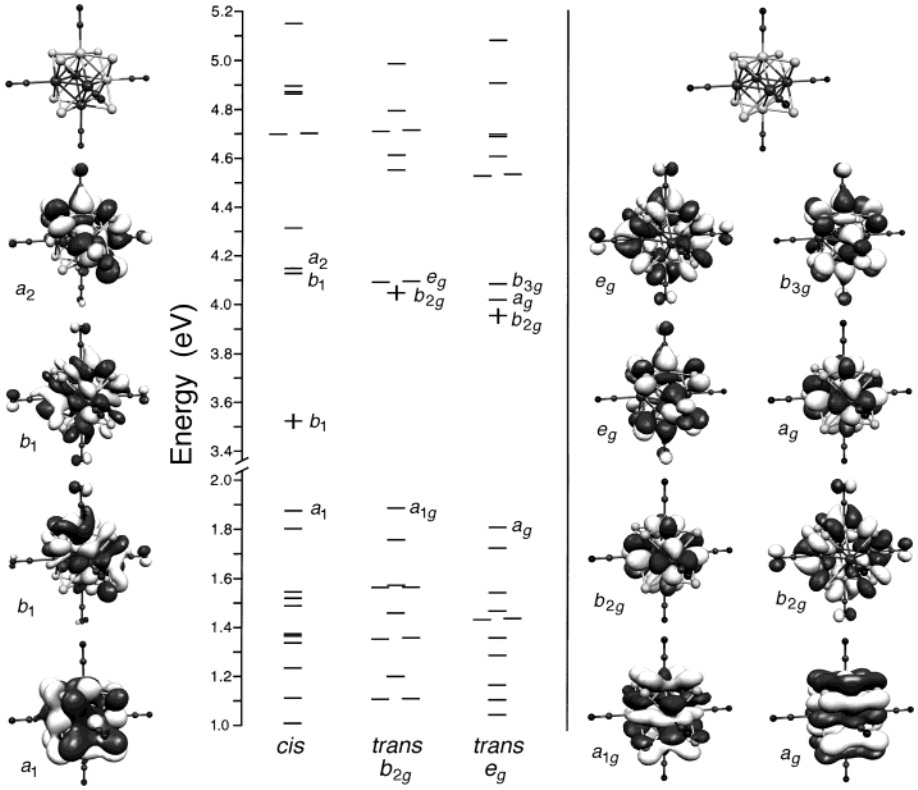

Figure 6. Energy level diagrams and frontier orbitals for the cis (left) and trans (middle and right) isomers of $[Re_4Os_2Se_8(CN)_6]^{3-}$, as calculated using DFT. SOMO levels are indicated by a vertical line, and all levels lower in energy are fully occupied. From bottom to top, the orbitals depicted correspond to the SOMO-1, SOMO, LUMO, and LUMO+1, respectively. Two low-lying states are shown for the trans isomer; the rightmost one (obtained by placing the unpaired electron in an e_g orbital) is the ground state and lies just 0.23 kcal/mol lower than the other state.

$Os_2Se_8(CN)_6]^{2-}$, possesses three closely spaced unoccupied orbitals that might receive the added electron: one b_{2g} orbital and a pair of e_g orbitals. Placing it in the b_{2g} orbital results in the central energy level diagram and frontier orbitals depicted in Figure 6. In this state, the b_{2g} SOMO is metal−metal antibonding in character, with no electron density arising on the cyanide ligands. Placing the electron instead in one of the e_g orbitals leads to a Jahn−Teller distorted state—corresponding to the rightmost energy level diagram and frontier orbitals in Figure 6—that is lower in energy by 0.23 kcal/mol.[34] Here, the SOMO has significant contributions from the π^* orbitals of four of the cyanide ligands, two of which are bound to osmium atoms. Note, however, that given their close proximity in energy, the unpaired electron can be anticipated to be nearly evenly distributed among the frontier b_{2g}, a_g, and b_{3g} orbitals at temperatures as low as 100 K. Furthermore, the character of these three orbitals is such as to place spin density in the π^* orbitals of all six cyanide ligands but particularly in those bound to the osmium atoms. In this situation, exchange coupling with *trans*-$[Re_4Os_2Se_8(CN)_6]^{3-}$ should also be strongest through the osmium-bound cyanide ligands.

Expanded Prussian Blue Analogues. Despite the differences in electronic structure at the osmium centers, mixed rhenium−osmium clusters can react to form porous solids in the same manner as do hexarhenium clusters. Addition of a soluble sodium salt such as NaSCN to an acetonitrile solution of $(Bu_4N)_3[Re_5OsSe_8(CN)_6]$ (**1**) induces precipitation of $Na_3[Re_5OsSe_8(CN)_6]$ (**2**). Directly paralleling the reactivity of $Na_3[Re_6Se_8(CN)_6]$,[9e] this water-soluble salt then reacts with nickel(II) in aqueous solution to yield an expanded Prussian blue type solid (**6**):

$$3[Ni(H_2O)_6]^{2+} + 2[Re_5OsSe_8(CN)_6]^{3-} \rightarrow Ni_3[Re_5OsSe_8(CN)_6]_2\cdot 32H_2O \quad (1)$$

As in the formation of $Ni_3[Re_6Se_8(CN)_6]_2\cdot 33H_2O$,[9e] the initial precipitate is poorly ordered but becomes more crystalline upon heating under the mother liquor at 80 °C for 14 h. A portion of the X-ray powder diffraction data for compound **6** is shown in Figure 7, together with a fit obtained using the Rietveld refinement method. The results confirm the expected Prussian blue type structure, in which alternating $[Re_5OsSe_8]^{3+}$ cluster cores and Ni^{2+} ions are connected through linear cyanide bridges to form a cubic lattice. Key interatomic distances and angles are listed in the legend of Figure 7 and do not differ significantly from those of $Ni_3[Re_6Se_8(CN)_6]_2\cdot 33H_2O$.[9e] As with this previous structure, one-third of the $[Re_5OsSe_8(CN)_6]^{3-}$ units are missing from the lattice, leading to a highly porous framework.

An analogous solid incorporating $[Re_4Os_2Se_8(CN)_6]^{3-}$ can be anticipated to behave as a microporous ferromagnet at low temperatures. Unfortunately, in aqueous solution, this 25-electron cluster rapidly oxidizes to give the diamagnetic 24-electron species $[Re_4Os_2Se_8(CN)_6]^{2-}$. Since crystalline Prussian blue analogues generally only form in aqueous reactions, the realization of such a material awaits development of a novel nonaqueous route to its assembly. Alternatively, synthesis of $[Re_3Os_3Se_8(CN)_6]^{2-}$ might provide a more stable 25-electron cluster for this purpose.

(34) A similar situation occurs for $[Re_5OsSe_8(CN)_6]^{4-}$, where placing the additional electron in an e orbital affords a state 0.95 kcal/mol lower in energy than that obtained by placing it in a nearby b_1 orbital. See Figure S1 in the Supporting Information for further details.

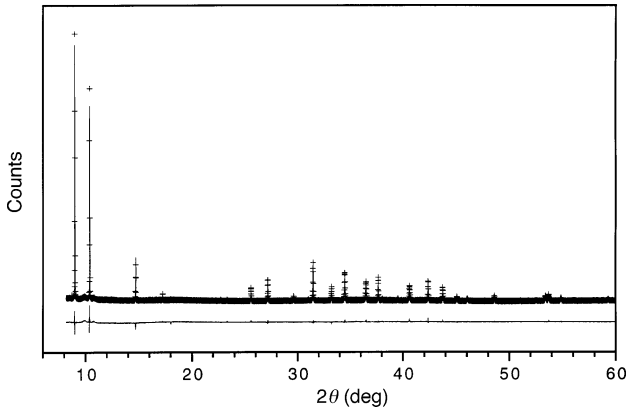

Figure 7. A portion of the powder X-ray diffraction data for compound **6** (crosses) along with the final fit from the crystallographic analysis (upper solid line). The lower solid line plots the difference between the observed and simulated patterns. Selected interatomic distances (Å) and angles (deg) from the refined structure: M−M 2.625(3), M−Se 2.506(2), M−C 2.05(1), C−N 1.15(1), Ni−N 2.02(2), Ni−O 2.432, Se−Re−C 91.9(1), Re−Re−Se 58.4(2), 118.4(2).

Hexacopper Cluster Assemblies. Discrete molecular assemblies were targeted as an alternative means of probing the propensity of the 25-electron clusters for engaging in magnetic exchange coupling. To prevent formation of an extended solid and minimize any potential interassembly exchange interactions, the tetradentate chelating ligand Me_6tren was employed as a blocking group. Copper(II) complexes of Me_6tren typically display a trigonal bipyramidal geometry, with an anion or solvent molecule occupying the fifth, axial coordination site.[21] Such an arrangement is well-suited for our purpose, since the spin-carrying d_{z^2} orbital interacts strongly with the apical ligands and can lead to strong magnetic exchange coupling through cyanide.[35]

Reaction of the 25-electron cluster $[Re_4Os_2Se_8(CN)_6]^{3-}$ with $[(Me_6tren)Cu(CF_3SO_3)]^+$ in acetonitrile generates the intended $\{Re_4Os_2Se_8[CNCu(Me_6tren)]_6\}^{9+}$ assembly. Figure 8 depicts its structure, as observed in crystals of $\{Re_4Os_2Se_8[CNCu(Me_6tren)]_6\}(CF_3SO_3)_9$·14MeCN (**9**·14MeCN). Therein, the geometry of the central $[Re_4Os_2Se_8(CN)_6]^{3-}$ unit is similar to that in $(PPh_4)_2(CoCp_2)[Re_4Os_2Se(CN)_6]$ (see Table 3), differing primarily in its shorter M−C distance of 2.050(9) Å and slightly more bent M−C−N angle of 176.1(8)°. The nitrogen end of each cyanide ligand occupies an axial site in the trigonal bipyramidal coordination environment of a Cu^{II} center, with a C−N−Cu angle of 169.2(7)°. Cyano-bridged assemblies with related core structures are known, including $\{Mo_6Cl_8[NC-Mn(CO)_2Cp]_6\}^{2-}$, $\{Re_6Se_8(CN)_5[CNMn(H_2O)_5]\}^{2-}$, *trans*-$\{Re_6Te_8(CN)_4[CNCu(en)_2]\}$, and *trans*-$\{Re_6Te_8(CN)_2[CNMn(OEP)]_4\}$, but none incorporate a paramagnetic cluster unit.[10c,36] Such species can be viewed as cluster-expanded variants of a rapidly growing set of $M(CN)_{6-n}(CNM')_n$ assemblies based upon simple hexacyanometalate complexes.[37]

Analogous constructs featuring 23- and 24-electron clusters were also sought for comparison. Parallel assembly reactions utilizing $[Re_6Se_8(CN)_6]^{3-}$ and $[Re_5OsSe_8(CN)_6]^{3-}$ in place of $[Re_4Os_2Se_8(CN)_6]^{3-}$ indeed afford $\{Re_6Se_8[CNCu(Me_6tren)]_6\}(CF_3SO_3)_9$ (**7**) and $\{Re_5OsSe_8[CNCu(Me_6tren)]_6\}(CF_3SO_3)_9$ (**8**). In each case, the cyanide stretching mode shifts toward higher frequency in the infrared spectrum, as expected when converting from a terminal to a bridging cyanide ligand. The solution-phase and solid-state infrared spectra are essentially identical, indicating that these assemblies remain intact in acetonitrile solution. Crystals of **8**·14MeCN were found to be isostructural with those of **9**·14MeCN.

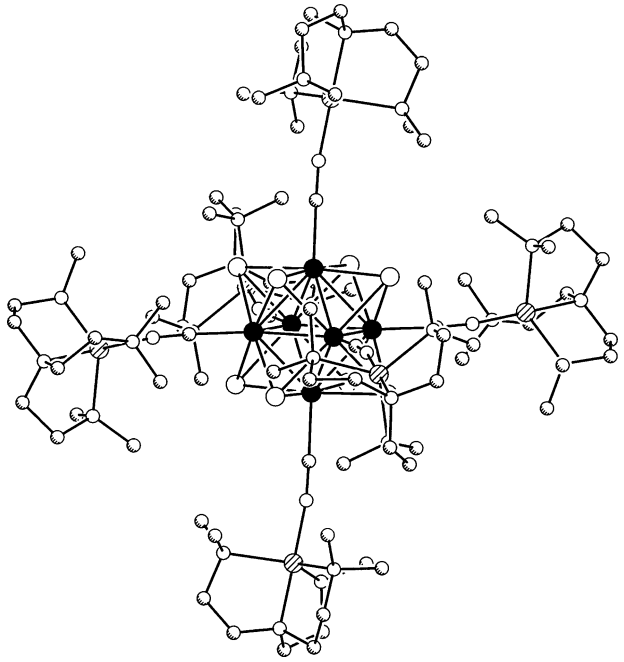

Figure 8. Structure of the $\{Re_4Os_2Se_8[CNCu(Me_6tren)]_6\}^{9+}$ assembly, as observed in **9**·14MeCN. Black, large white, shaded, small white, and hatched spheres represent M (=Re or Os), Se, C, N, and Cu atoms, respectively. The molecule resides on a $\bar{3}$ symmetry site in the crystal. Selected interatomic distances (Å) and angles (deg) for **8**·14MeCN and **9**·14MeCN, respectively: mean M−M 2.623(2), 2.651(1), mean M−Se 2.513(2), 2.514(1), M−C 2.07(2), 2.050(9), C−N 1.16(2), 1.17(1), N−Cu 1.93(2), 1.922(7), M−C−N 175(2), 176.1(8), C−N−Cu 169(2), 169.2(7).

Magnetic susceptibility data were collected for compounds **7**−**9** to check for magnetic exchange coupling between their respective 23-, 24-, and 25-electron clusters and the surrounding Cu^{II} centers. In each case, the data were corrected for an anomalous magnetic response of the type commonly encountered for weakly paramagnetic copper(II) compounds.[38] Figure 9 shows the temperature dependence of $\chi_M T$ for all three compounds. The moments observed at room temperature are all reasonable for samples with six or seven $S = {}^1/_2$ centers per formula unit, in the absence of any exchange coupling.

(35) Bieksza, D. S.; Hendrickson, D. N. *Inorg. Chem.* **1977**, *16*, 924.
(36) (a) Johnston, D. H.; Stern, C. L.; Shriver, D. F. *Inorg. Chem.* **1993**, *32*, 5170. (b) Naumov, N. G.; Artemkina, S. B.; Virovets, A. V.; Fedorov, V. E. *J. Solid State Chem.* **2000**, *153*, 195. (c) Mironov, Y. V.; Fedorov, V. E.; Ijjaali, I.; Ibers, J. A. *Inorg. Chem.* **2001**, *40*, 6320.
(37) (a) Scuiller, A.; Mallah, T.; Verdaguer, M.; Nivorozkhin, A.; Tholence, J. L.; Veillet, P. *New J. Chem.* **1996**, *20*, 1. (b) Miyasaka, H.; Matsumoto, N.; Okawa, H.; Re, N.; Gallo, E.; Floriani, C. *J. Am. Chem. Soc.* **1996**, *118*, 981. (c) Parker, R. J.; Hockless, D. C. R.; Moubaraki, B.; Murray, K. S.; Spiccia, L. *Chem. Commun.* **1996**, 2789. (d) Miyasaka, H.; Ieda, H.; Matsumoto, N.; Re, N.; Crescenzi, R.; Floriani, C. *Inorg. Chem.* **1998**, *37*, 255. (e) Arrio, M. A.; Scuiller, A.; Sainctavit, P.; Moulin, C. C. D.; Mallah, T.; Verdaguer, M. *J. Am. Chem. Soc.* **1999**, *121*, 6414. (f) Parker, R. J.; Spiccia, L.; Batten, S. R.; Cashion, J. D.; Fallon, G. D. *Inorg. Chem.* **2001**, *40*, 4696. (g) Shen, X.; Li, B.; Zou, J.; Xu, Z. *Transition Met. Chem.* **2002**, *27*, 372. (h) Parker, R. J.; Spiccia, L.; Moubaraki, B.; Murray, K. S.; Hockless, D. C. R.; Rae, A. D.; Willis, A. C. *Inorg. Chem.* **2002**, *41*, 2489. (i) Marvaud, V.; Decroix, C.; Scuiller, A.; Guyard-Duhayon, C.; Vaissermann, J.; Gonnet, F.; Verdaguer, M. *Chem.—Eur. J.* **2003**, *9*, 1678. (j) Marvaud, V.; Decroix, C.; Scuiller, A.; Tuyéras, F.; Guyard-Duhayon, C.; Vaissermann, J.; Marrot, J.; Gonnet, F.; Verdaguer, M. *Chem.—Eur. J.* **2003**, *9*, 1692. (k) Choi, H. J.; Sokol, J. J.; Long, J. R. *J. Phys. Chem. Solids*, in press.
(38) Escuer, A.; Ribas, J. *J. Chem. Soc., Dalton. Trans.* **2002**, 3778.

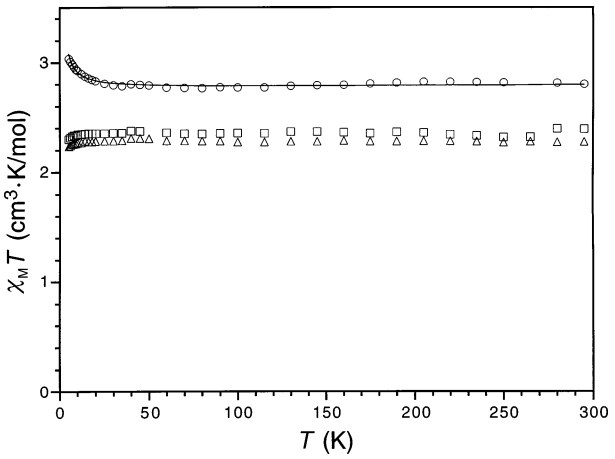

Figure 9. Variable-temperature magnetic data for compounds **7** (squares), **8** (triangles), and **9** (circles), as measured in an applied field of 1000 G.

Essentially no variation in $\chi_M T$ is observed for compounds **7** and **8** at temperatures down to 5 K, indicating the lack of any appreciable magnetic exchange coupling. In the former case, this occurs despite the presence of the paramagnetic 23-electron cluster $[Re_6Se_8(CN)_6]^{3-}$, owing to the aforementioned symmetry of its SOMO. In the latter case, this is due to the diamagnetism of 24-electron $[Re_5OsSe_8(CN)_6]^{3-}$ and the large separations between paramagnetic Cu^{II} centers. For compound **9**, however, $\chi_M T$ climbs steadily at temperatures below 30 K, signaling the presence of ferromagnetic coupling between 25-electron $[Re_4Os_2Se_8(CN)_6]^{3-}$ and at least some of the surrounding Cu^{II} centers. The coupling is clearly quite weak, but its ferromagnetic nature is consistent with the orthogonality of the calculated SOMOs discussed above and the axially extending d_{z^2} spin−orbital of the trigonal bipyramidal Cu^{II} centers.[14] To our knowledge, this is the first demonstration of magnetic coupling involving such a hexanuclear cluster unit.

An estimate of the strength of the exchange coupling in $\{Re_4Os_2Se_8[CNCu(Me_6tren)]_6\}^{9+}$ was obtained by fitting the magnetic data using MAGFIT 3.1[39] and an exchange Hamiltonian of the following form:

$$\hat{H} = -2J[\hat{S}_{Re_4Os_2}\cdot(\hat{S}_{Cu(1)} + \hat{S}_{Cu(2)} + \hat{S}_{Cu(3)} + \hat{S}_{Cu(4)} + \hat{S}_{Cu(5)} + \hat{S}_{Cu(6)})] \quad (2)$$

The best fit gave $g = 2.05$ and $J = 0.4$ cm^{-1} and corresponds to the solid line in Figure 9. Identical values were obtained by fitting data collected in a 10 kG field instead of a 1 kG field. With this model, the assembly would be predicted to have an $S = {}^7/_2$ ground state. Note, however, that the system is actually much more complicated than suggested by the foregoing exchange Hamiltonian, in which all cluster−copper exchange interactions are treated as equivalent. In reality, the compound consists of 33% *cis*-$\{Re_4Os_2Se_8[CNCu(Me_6tren)]_6\}^{9+}$ and 67% *trans*-$\{Re_4Os_2Se_8[CNCu(Me_6tren)]_6\}^{9+}$. On the basis of the calculated SOMOs for the central cluster units of these two isomers (see Figure 6), one would expect the former to display coupling primarily to just the two Cu^{II} centers attached to osmium and the latter to display coupling to just four of the surrounding Cu^{II} centers. Thus, at least along an Os−CN−Cu pathway, the true coupling constant is likely somewhat higher than the crude estimate of $J = 0.4$ cm^{-1}.

Outlook

The foregoing results demonstrate the ability of a face-capped octahedral cluster with 25 metal-based valence electrons—specifically, $[Re_4Os_2Se_8(CN)_6]^{3-}$ to participate in magnetic exchange coupling. The observed ferromagnetic coupling with appended Cu^{II} centers is weak, most likely as a consequence of the cluster spin being diluted over its sizable core. Analogous clusters with $S > {}^1/_2$ can be expected to provide stronger exchange coupling by projecting greater spin density onto the outer ligands. Indeed, the cyclic voltammograms and DFT calculations reported here point toward the possibility of isolating a 26-electron $[Re_3Os_3Se_8(CN)_6]^{3-}$ cluster with an $S = 1$ ground state. Other promising candidates for this purpose include potential hexacyanide species containing $[Fe_6S_8]^{n+}$, $[Zr_6ZX_{12}]^{n+}$ (Z = interstitial main group or transition element; X = Cl, Br, I), and $[Gd_6ZX_{12}]^{n-}$ cores.[13b,20d,40] Ultimately, it is hoped that the realization of such molecules will lead to a material with a highly porous magnetic framework.

Acknowledgment. This research was funded by NSF Grant No. CHE-0111164, DOE Grant No. DE-FG03-01ER15257, and the France-Berkeley Fund. We thank Atofina Chemical Inc. for partial support of E.G.T. and N.R.M.C., Dr. V. Yachandra for helpful discussions, Prof. A. M. Stacy for use of the SQUID magnetometer, and Prof. D. N. Hendrickson for supplying software used to fit the magnetic susceptibility data. A portion of this research was carried out at the Stanford Synchrotron Radiation Laboratory, which is operated by the Department of Energy, Office of Basic Energy Science.

Supporting Information Available: Results from the DFT calculations on $[Re_5OsSe_8(CN)_6]^{4-}$ (PDF) and an X-ray crystallographic file (CIF). This material is available free of charge via the Internet at http://pubs.acs.org.

JA037444Q

(39) Schmitt, E. A. Ph.D. Thesis, University of Illinois, 1995.

(40) Selected lead references: (a) Simon, A. *Angew. Chem., Int. Ed. Engl.* **1988**, *27*, 159. (b) Lee, S. C.; Holm, R. H. *Angew. Chem., Int. Ed. Engl.* **1990**, *29*, 840. (c) Corbett, J. D. *J. Alloys Cmpds.* **1995**, *229*, 10.